H_∞ CONTROL OF ROBOT ARM WITH HYDRAULIC DRIVE

Zdzisław GOSIEWSKI[*], Grzegorz MICHAŁOWSKI[*]

[*] Faculty of Mechanical Engineering, Białystok Technical University, ul. Wiejska 45 C, 15-351 Białystok

gosiewski@pb.edu.pl, g.m@onet.eu

Abstract: In the paper an H_∞ velocity control of the robot arm in combination with the hydraulic drive is presented. The open-loop system consists of a manipulator with one rotary degree of freedom, a hydraulic servomotor, and an electrohydraulic amplifier. The mathematical model of the system is derived. Due to the nonlinearity in the model, which is caused by varying operating point parameters and the direction of the servomotor motion, the model of multiplicative uncertainty was defined. The plant model transfer function parameters were assumed to be variable. To limit error signal, control signal, and output signal three weighting functions were designed. The simulation results of the designed H_∞ optimal closed-loop system were compared to the standard PID closed-loop system. The solution ensuring robust performance was achieved and proved.

1. INTRODUCTION

Nowadays, industrial robots (manipulators) are widely used in manufacturing tasks. The manipulators are driven by hydraulic servomotors, and there is an obvious need to achieve robust performance in case of, for example, varying parameters that describe such systems. These factors influence on time and frequency quality of the system, and the standard control methods may not be sufficient in such cases. Thus, in this paper the H_∞ robust control is analyzed. The considered system consists of three main elements: the manipulator, which angular velocity is to be controlled, the hydraulic servomotor, and the electrohydraulic amplifier as an actuator. Models of these elements are combined to form the plant model with uncertain values of the transfer function parameters. The servomotor with the manipulator is a simplified, plane mechanism with one rotary degree of freedom. To obtain a simple model of the plant some simplifications were necessary. Moment of inertia of the servomotor, clearance between joints, and friction forces were omitted. Additionally, the stiffness of the structure was assumed to be infinite. Design procedure of the H_∞ robust controller requires the model of uncertainty and the weighting functions to be included, thus, they are to be designed. Every transfer function presented in the article is taken to be a function of s, therefore the (s) notation will be dropped henceforth.

2. CONTROL PLANT

All the considered elements of the open-loop system have been identified in (Henzel, 2004) and (Cedro, 2007). The first element of the plant is the electrohydraulic amplifier with the following 2nd-order transfer function:

$$G_1 = \frac{4800}{s^2 + 400\,s + 48000} \quad \text{(Henzel, 2004).} \tag{1}$$

The model of the servomotor with the manipulator, shown in Fig. 1, has been experimentally derived and has the general 2nd-order form with three varying parameters:

$$G_2 = \frac{b_0}{s^2 + a_1\,s + a_0} \quad \text{(Cedro, 2007).} \tag{2}$$

The possible values of parameters: b_0, a_1 and a_0, depending on the operating point parameters, have been determined as well (Fig. 2). Due to the structural constraints, the rotational angle of the robot arm can vary from 0.4 to 1.5 rad.

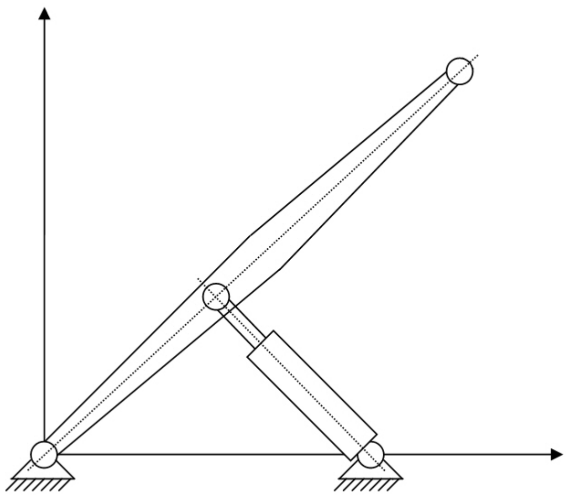

Fig. 1. Sample configuration of servomotor and manipulator with one rotary degree of freedom

Introduced elements are combined to form the open-loop system model, which is assumed to be the product of transfer function of the actuator (1) and transfer function of the servomotor/arm (2) with three varying parameters, and it has the following 4th-order form:

$$G = \frac{4800}{s^2 + 400s + 48000} \cdot \frac{b_0}{s^2 + a_1 s + a_0}. \tag{3}$$

The voltage is the input signal to the plant, and the angular velocity of the robot arm, φ_0, is the output signal. The displacement of the hydraulic piston, x_0 is the transitional signal between amplifier and servomotor.

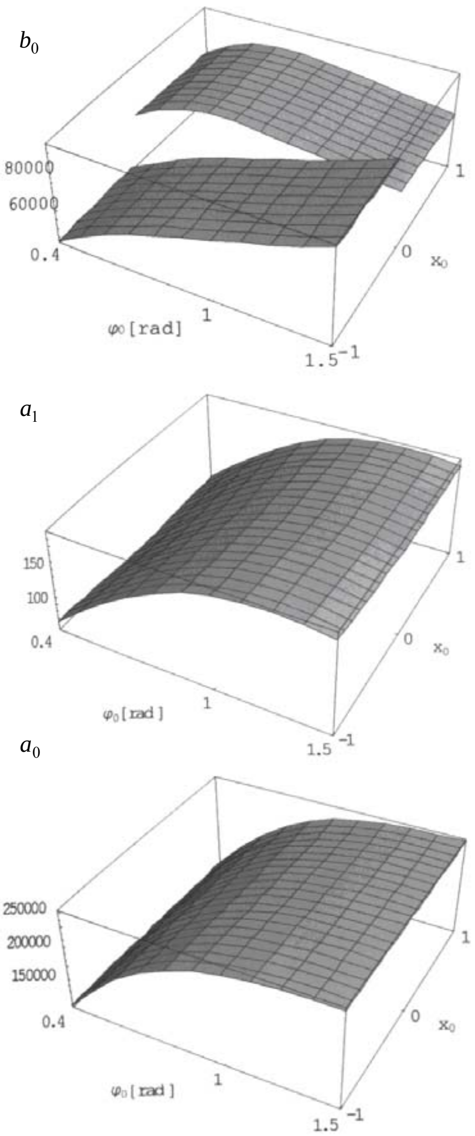

Fig. 2. Relationship between plant model parameters and operating point parameters, φ_0 – rotational angle of the robot arm, x_0 – displacement of the hydraulic piston (Henzel, 2004)

To reduce the number of considered variants resulting from (3) and Fig. 2, the nominal (4), the minimal (5), and the maximal (6) transfer functions were defined as follows:

$$G_0 = \frac{4800}{s^2 + 400s + 48000} \cdot \frac{65000}{s^2 + 125s + 175000}, \tag{4}$$

$$G_{\min} = \frac{4800}{s^2 + 400s + 48000} \cdot \frac{40000}{s^2 + 50s + 100000}, \tag{5}$$

$$G_{\max} = \frac{4800}{s^2 + 400s + 48000} \cdot \frac{90000}{s^2 + 200s + 250000}. \tag{6}$$

The nominal plant model was assumed to be the transfer function with parameters: b_0, a_1, and a_0, calculated as the arithmetic mean of their extreme values. The minimal and the maximal plant models were taken to have respectively minimal and maximal values of the transfer function parameters: b_0, a_1, and a_0. Notice that the maximal model has the least gain (Figs. 3, 4).

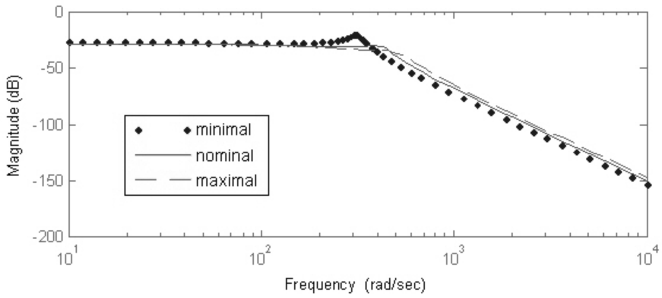

Fig. 3. Magnitude-frequency plots of the nominal, the minimal, and the maximal plant model

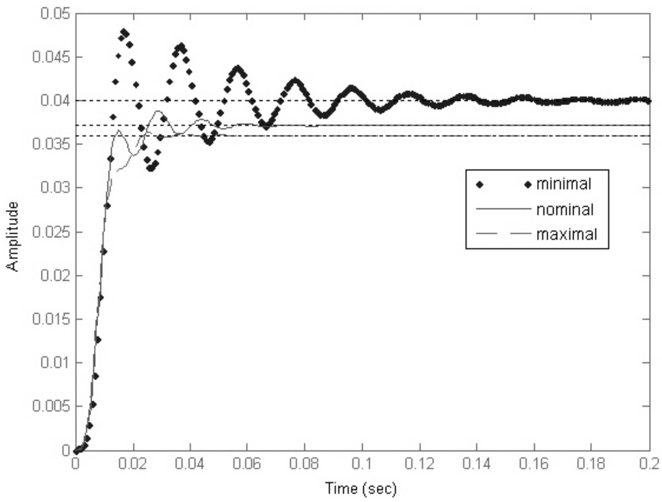

Fig. 4. Step responses of the nominal, the minimal, and the maximal plant model

3. DESIGN PROCESS OF H_∞ ROBUST CONTROL SYSTEM

The H_∞ robust control problem is to achieve such K controller that provides minimization of the H_∞ norm of the considered closed-loop system described by the transfer function $F(G, K)$, where G is the plant model:

$$\|H\|_\infty = \sup_{\omega \in R} \left(F(G, K)(j\omega) \right). \tag{7}$$

H_∞ norm is the supremum (upper bound) of the maximum singular value of the closed-loop system represented in the frequency domain.

3.1. Design process of PID controller

The design of the PID controller is based on the nominal plant model G_0 and is required to obtain the sensitivity function, the control function, and the complementary sensitivity function, which are essential to the further weighting functions design. The ideal PID controller parameters were selected to achieve zero overshoot and sufficiently short settling time of the closed-loop system:

$$K_{\mathrm{PID}} = K_{\mathrm{p}}\left(1+\frac{1}{T_{\mathrm{i}}s}+T_{\mathrm{d}}s\right) = 10\left(1+\frac{1}{0.01s}+0.001s\right), \tag{8}$$

where: K_{p} – proportional gain, T_{i} – integral time, T_{d} – derivative time.

The transfer function (8) was then approximated by the proper transfer function of the physically realizable PID controller that is described as follows:

$$K_{\mathrm{PID}} = 10\left(1+\frac{1}{0.01s}+\frac{0.001s}{0.001s+1}\right). \tag{9}$$

3.2. Weighting functions

The first requirement of the H_∞ robust controller design procedure is the proper choice of the weighting functions that limit the error signal, the control signal, and the output signal. For the purpose of the robust design three weighting functions W_{e}, W_{u}, and W_{y} were designed. They are based on the sensitivity function, the control function, and the complementary sensitivity function, respectively:

$$S = \left(I + K\,G_0\right)^{-1}, \tag{10}$$

$$R = K\left(I + K\,G_0\right)^{-1}, \tag{11}$$

$$T = K\,G_0\,S\,, \tag{12}$$

where K was taken to be K_{PID} (9). The designed weighting functions have the forms:

$$W_{\mathrm{e}} = \frac{8.5s+100}{30s+0.1}, \tag{13}$$

$$W_{\mathrm{u}} = \frac{s+22}{22s+720}, \tag{14}$$

$$W_{\mathrm{y}} = \frac{s+1500}{0.1s+1500}. \tag{15}$$

Magnitude-frequency plots of the weighting functions (13)–(15) with corresponding system functions for standard PID closed-loop system are presented in Fig. 5.

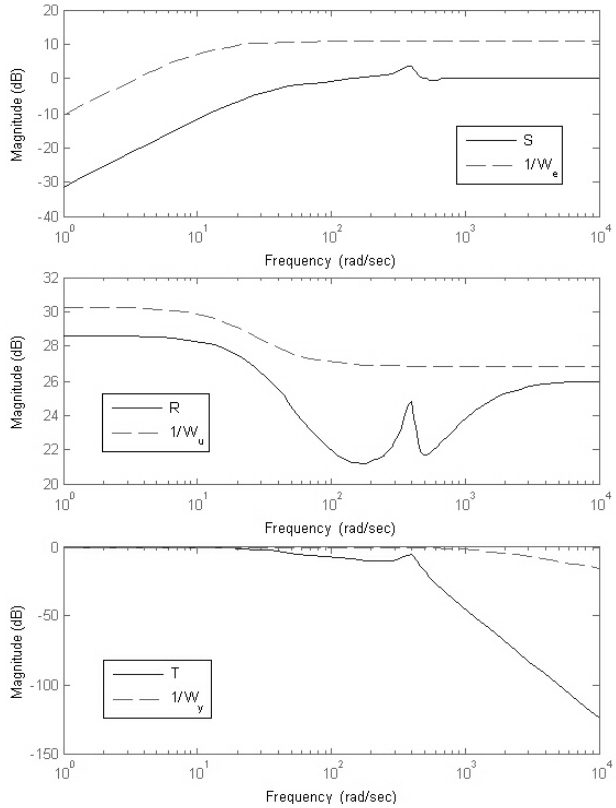

Fig. 5. Magnitude-frequency plots of the weighting functions W_{e}, W_{u}, W_{y} and corresponding standard PID system functions

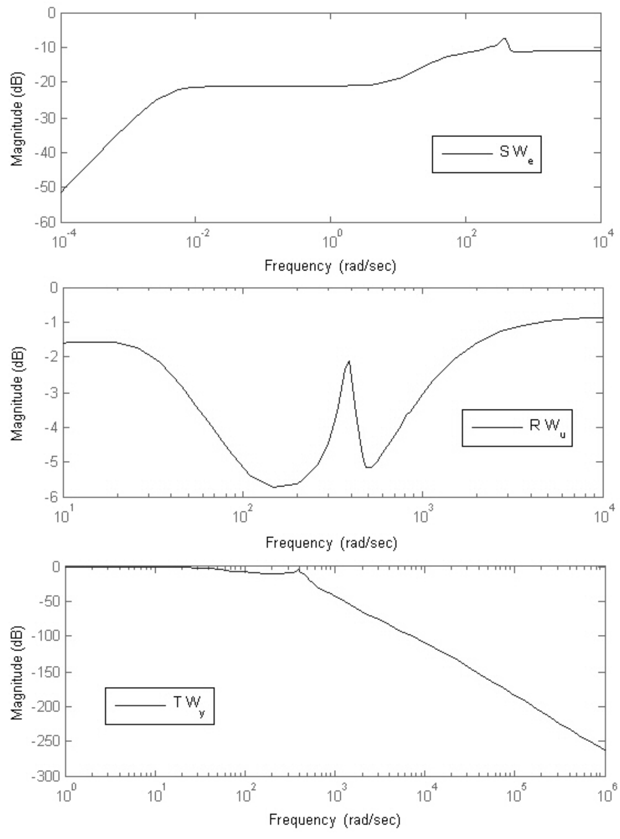

Fig. 6. Graphic interpretation of the conditions (16)–(18)

Weighting functions are properly designed since they satisfy conditions:

$$\left|W_e(j\omega)S(j\omega)\right| \le 1, \quad \forall\omega, \tag{16}$$

$$\left|W_u(j\omega)R(j\omega)\right| \le 1, \quad \forall\omega, \tag{17}$$

$$\left|W_y(j\omega)T(j\omega)\right| \le 1, \quad \forall\omega. \tag{18}$$

The maximal gain of the considered products does not exceed the magnitude of 1, which in the logarithmic scale equals 0 dB, for every case (Fig. 6).

3.3. Model of uncertainty

The second requirement of the H_∞ controller design procedure is connected with the definition of uncertainty. The robust controller should ensure sufficient time and frequency quality of the closed-loop system even in case of the difference between the real plant and its assumed nominal model. In general, there are two kinds of uncertainty models: additive and multiplicative, which we define as follows:

$$\Delta_A = G_{max} - G_0, \tag{19}$$

$$\Delta_M = \frac{G_{max} - G_0}{G_0}. \tag{20}$$

Thus, the nominal model of the plant with each uncertainty will have the general form, respectively:

$$G_A = G_0 + \Delta_A, \tag{21}$$

$$G_M = G_0 \cdot (1 + \Delta_M). \tag{22}$$

In both cases, the 8th-order uncertainty model is produced. To check the differences between each interconnection to the nominal plant model, consider Fig. 7.

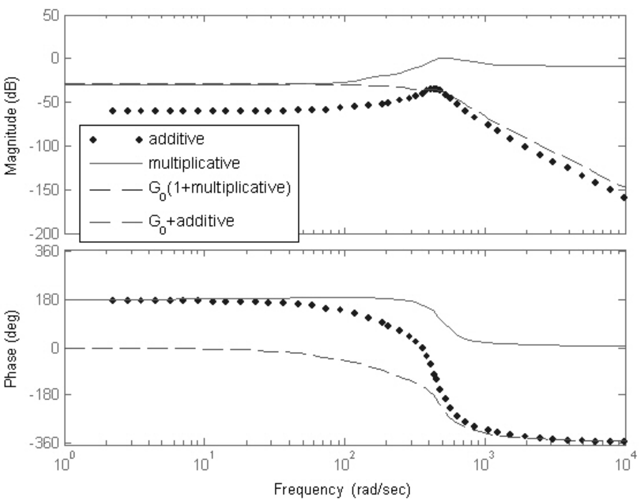

Fig. 7. Bode plots of additive and multiplicative uncertainty models, and their interconnection to the nominal plant model

It is shown that there is no difference between each interconnection (two dashed lines agree with each other), thus, to include varying model parameters the multiplicative uncertainty was chosen (22, Fig. 8b).

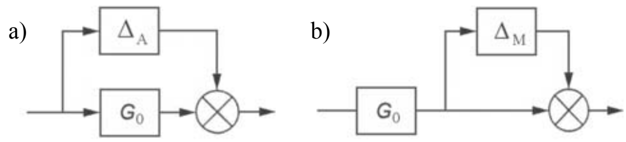

Fig. 8. Representation of additive (a) and multiplicative (b) uncertainty

3.4. Design process of H_∞ controller

To obtain the H_∞ robust controller a plant augmentation is required. The expanded model includes 4th-order nominal plant model G_0, 8th-order multiplicative uncertainty Δ_M, and three of 1st-order weighting functions W_e, W_u, W_y what produces 15th-order augmented plant model. Due to the above, the designed controller is described by 15th-order transfer function as well. Therefore, to reduce system complexity, the controller reduction should be applied. To do it, the *Hankel Singular Values* method was used. This technique estimates the "energy" of each controller state, keeping major states and discarding the minor ones. Keeping larger "energy" states of the controller preserves most of its characteristics in terms of stability, frequency, and time responses (Balas et al., 2007). Due to the only one dominant state in this case, the 14 states were safely rejected (Fig. 9).

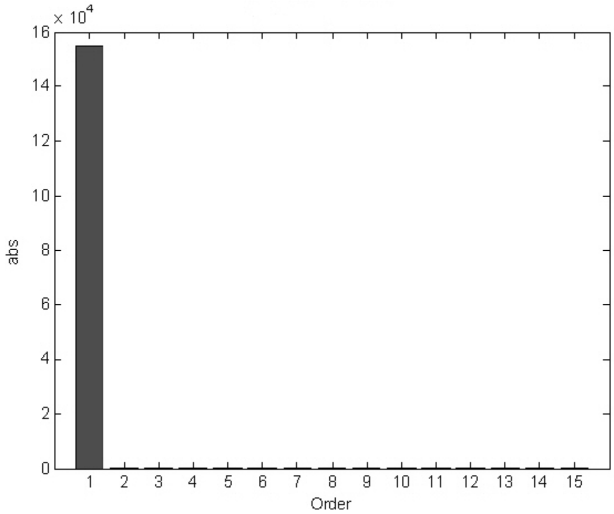

Fig. 9. Hankel singular value plot of the 15th-order controller

Thus, the H_∞ robust controller can be simplified to the 1st-order transfer function:

$$K = \frac{1033}{s + 0.003334}. \tag{23}$$

The time-domain comparison between 15th-order robust controller, reduced 1st-order robust controller, and standard PID controller (9) is shown in Fig. 10.

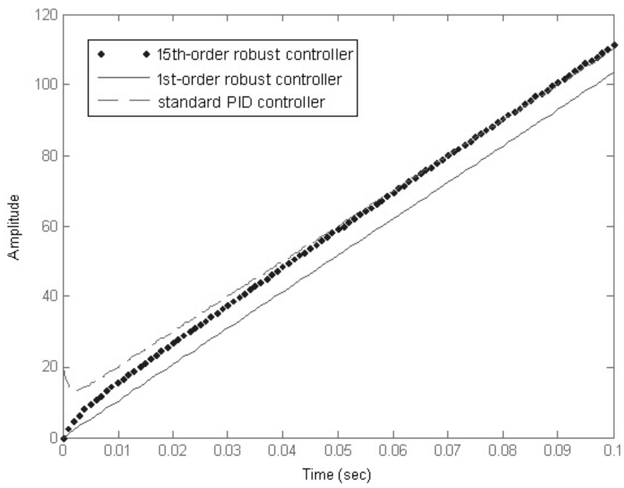

Fig. 10. Step responses: 15th-order robust controller, reduced 1st-order robust controller, and standard PID controller

It is shown that in the transient state of the closed-loop system the reduced robust controller acts as an integrator, and due to its very high gain the steady-state error is almost equal to zero. This can be proved using the *Final Value Theorem* (Franklin et al., 2002).

To determine the H_∞ system functions *S*, *R*, *T* the designed robust controller (23) can be substituted for *K* in equations (10)–(12). Magnitude-frequency plots of the weighting functions (13)–(15) with corresponding H_∞ system functions are presented in Fig. 11.

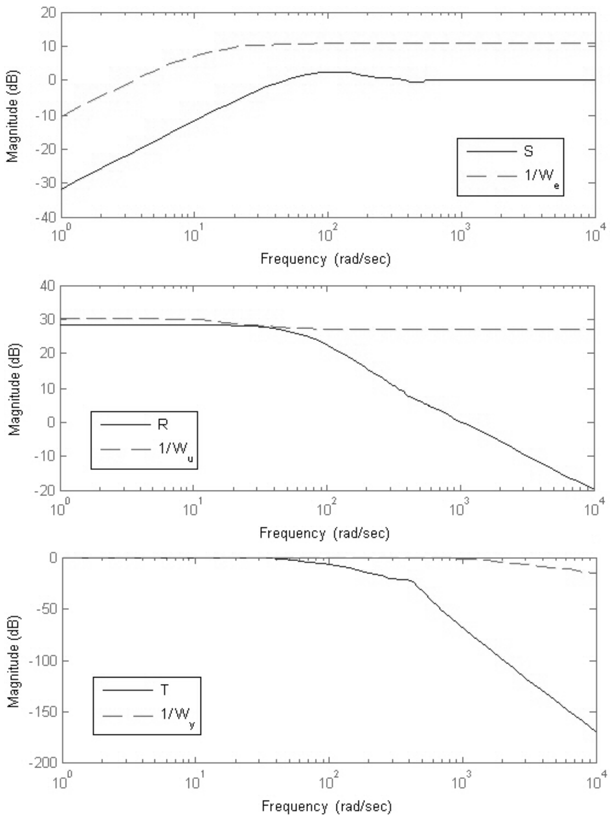

Fig. 11. Magnitude-frequency plots of the weighting functions W_e, W_u, W_y and corresponding H_∞ system functions

The comparison between Figs. 5 and 11 shows that the H_∞ system functions do not contain as high resonant peaks for some frequency as the standard PID system functions, what is the result of the H_∞ norm minimization.

The comparison between step responses of the designed H_∞ closed-loop system and the PID closed-loop system for the uncertainty model is shown in Fig. 12.

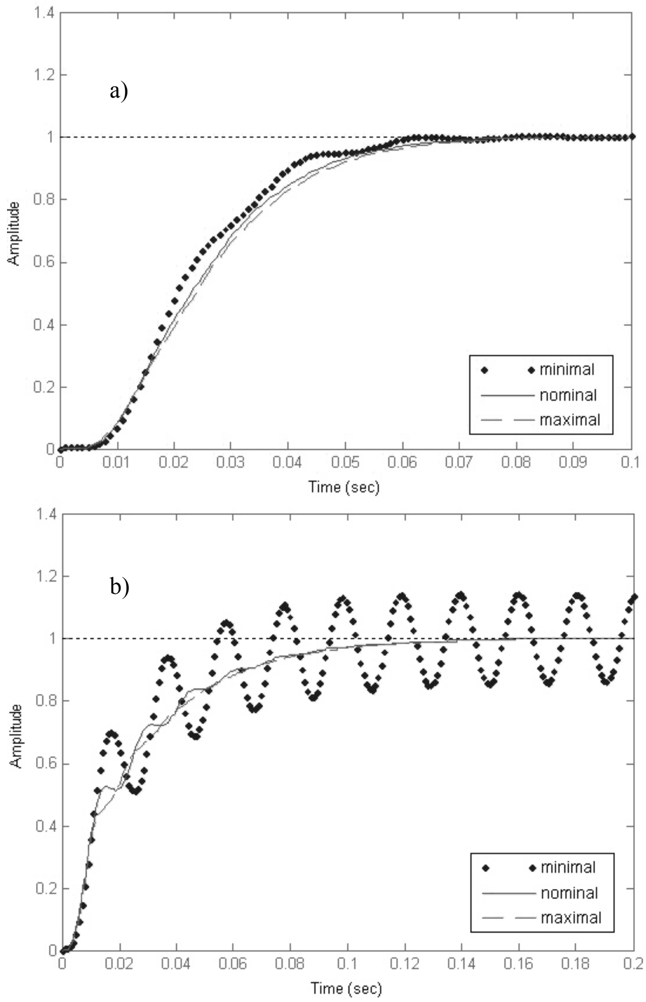

Fig. 12. Step responses: H_∞ closed-loop system (a), PID closed-loop system (b)

The investigated dynamic responses show that the H_∞ closed-loop system achieves better time-domain quality than the PID closed-loop system, since there is no overshoot and settling time is sufficiently short for each plant model with extreme values of varying parameters. Using standard PID control in this case can lead to oscillations of the output signal. Thus, PID controller might not provide stability of the system with, for example, higher ranges of varying parameters.

The comparison between frequency responses of the H_∞ closed-loop system and the PID closed-loop system for the uncertainty model is shown in Fig. 13.

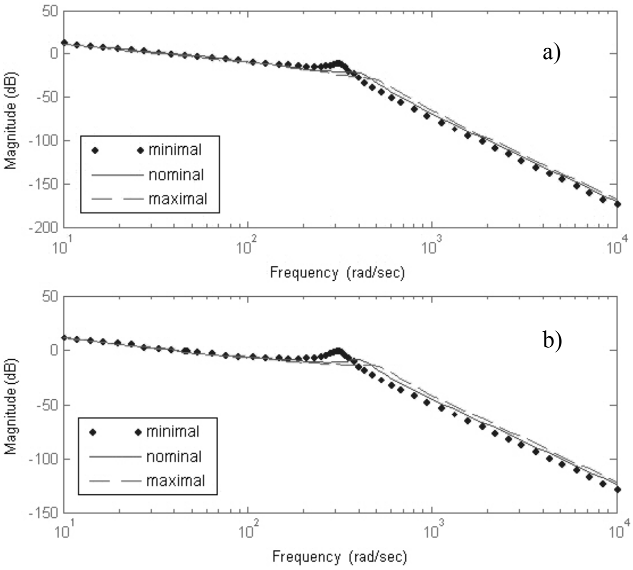

Fig. 13. Magnitude-frequency plots: H_∞ closed-loop system (a), PID closed-loop system (b)

The investigated responses show that the H_∞ closed-loop system achieves better frequency-domain quality than PID closed-loop system, since there is higher high-frequency decrease than in the standard PID closed-loop system. Therefore, the robust control system can more effectively attenuate sensor noises and other high-frequency disturbances, which could otherwise shift themselves to lower frequencies.

4. CONCLUSION

In the paper the H_∞ robust control method was applied to control the robot arm angular velocity. Due to time-varying plant model parameters, the multiplicative uncertainty model was defined. To satisfy the H_∞ robust controller design procedure requirements, three weighting functions were taken into account as well. The time and frequency responses of the robust control system and the standard PID closed-loop system were investigated. The H_∞ robust system showed better quality and manifested robust performance in spite of uncertainties in the plant model.

REFERENCES

1. **Balas G.**, **Chiang R., Packard A., Safonov M.** (2007), *Robust Control Toolbox*. *User's Guide*, The MathWorks Inc.
2. **Cedro L.** (2007), *Identification of the systems with hydraulic drives by using of differential filters* (in Polish), Ph.D. Thesis, Kielce University of Technology.
3. **Dorf R.C., Bishop R.H.** (2005), *Modern Control Systems*, 10th Edition, Prentice Hall.
4. **Franklin G.F., Powell J.D., Emami-Naeini A.** (2002), *Feedback Control of Dynamic Systems*, 4th Edition, Prentice Hall.
5. **Gosiewski Z., Mystkowski A.** (2006), One-DoF robust control of shaft supported magnetically, *Archives of Control Sciences*, Vol. 16, No. 3, 327–339.
6. **Henzel M.** (2004), *New control methods of aircraft's electrohydraulic servodrive* (in Polish), Ph.D. Thesis, Military University of Technology, Warsaw.
7. **Zhou K., Doyle J.C.** (1998), *Essentials of Robust Control*, Prentice Hall.